A Development of a New Mechanism of an Autonomous Unicycle

Ryo NAKAJIMA *, Takashi TSUBOUCHI *, Shin'ichi YUTA *, and Eiji KOYANAGI **
* Intelligent Robot Laboratory,
Institute of Information Science and Electronics,
University of Tsukuba,
1-1-1 Tennoudai, Tsukuba, Ibaraki, 305 JAPAN
E-mail:{tsubo, yuta}roboken.esys.tsukuba.ac.jp
** Yokosuka Technical Highschool,
4-10 Kugo-machi, Yokosuka, Kanagawa, 238 JAPAN,

Abstract

We propose a new mechanism of a unicycle. One feature of this robot is the shape of a wheel which is similar to a rugby ball. The other feature is that the body is separated into upper and lower parts. In this paper, we show the details of a mechanism of the robot, simple controller system, and some results of the performance experiment using designed controller. We present an experimental results that the robot can move straight and steer itself by proposed mechanism.

I. Introduction

We have long been developing a series of self-contained autonomous mobile robots since 1977, whose family name is "Yamabico" [1, 2, 3].

The standard "Yamabico" type robot has PWS (Powered Wheel Steering) kinematics. Normally, it has two casters in front and rear to support the body for stability. One of our technical interests is to stabilize a body without such casters. In fact, our research project developed a control configured type mobile robot – an inverse pendulum mobile robot [4]. This robot has powered wheels in the left and right without casters. One advantage of this type is not to get irregular disturbance from casters. It is necessary even for such a control configured mobile robot to move around the given track in two dimensional plane freely while keeping balance. This inverse pendulum type mobile robot could follow a sequence of line and circular trajectory segments [4].

Motivated by our research experiments on the inverse pendulum type mobile robot, we become more interested in such a control configured type vehicle that has only one powered wheel – *unicycle*. It is difficult even for humans to manage such a unicycle well because of its unstableness. Effective control is required to stabilize the unicycle. Osaka *et al.* developed a unicycle [6] in 1981. Their robot has a large arm sticking out to right and left side, and the lateral movement is stabilized by moving a weight along the arm. Honma *et al.* presented a unicycle which has large gyroscope spinning fast at the top of the body, whose posture is stabilized with controlled precession of the gyroscope [7]. Brown *et al.* presented a single-wheel robot [8]. Their robot has a large tire and stabilization mechanisms are inside of the wheel. Unfortunately, these precedent works were, however, concentrated on the stabilization control, and not so much on navigation in the two dimensional space.

Our emphasis besides technical interests are not only stabilization of the unicycle but also navigation, *i.e.* we desire even the unicycle to be able to track a given trajectory which is specified by a combination of lines and circles. From this point of view, we designed a new mechanism of an autonomous unicycle robot. A prototype of our newly designed unicycle robot has been built as an experimental setup. In this report, an implementation of the posture and velocity control system of this robot and some "toddling" experiments are illustrated.

II. A new mechanism of a unicyle

Our designed mechanism of the unicycle is illustrated in Fig. 1. Let us define a coordinate system on the unicycle with x, y and z axes as shown in (Fig. 1). The origin of the coordinate system is placed at the center of the joint. x, y and z axis are parallel to the front-rear, left-right, and vertical directions respectively. We use "*roll* " or "*rolling*" as an angular motion about the x axis, "*pitch*" or "*pitching*" about the y axis, and "*yaw*" or "*yawing*" about the z axis.

The wheel shape which is similar to a rugby ball is a distinctive feature of the proposed unicycle robot. This wheel shape helps to keep its *rolling* stability to a large extent, because the robot can behave as if it were a "*tumbler doll*" if the center of mass of the robot is lower than the center of the wheel arc of the cross

Proc. IROS 97 0-7803-4119-8/97/$10©1997 IEEE

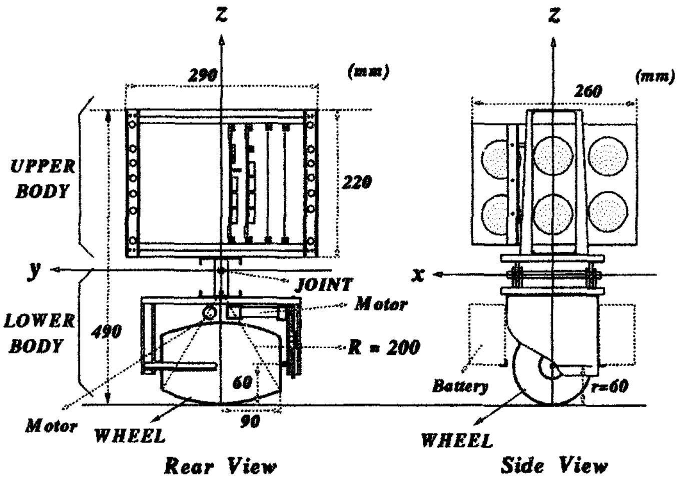

Figure 1: The illustrated design of the unicycle

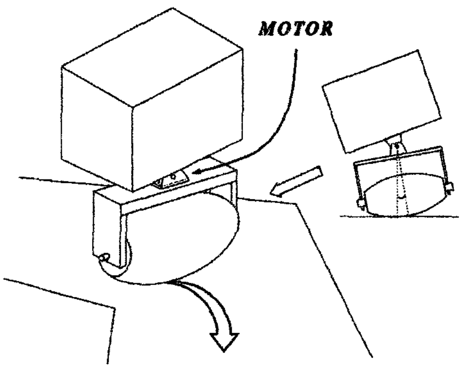

Figure 2: Steering method using *rolling* the upper side body

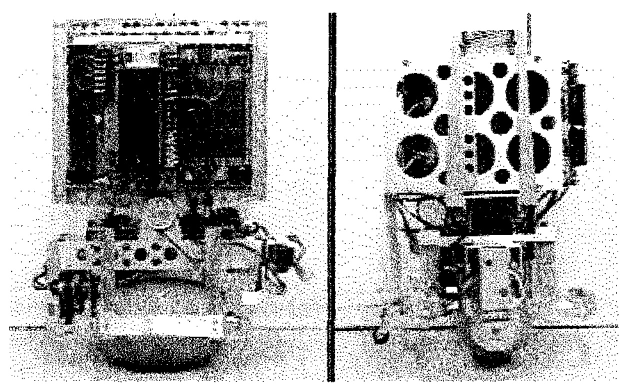

Figure 3: The unicycle robot Yamabico ICHIRO

section along an axle of the wheel. In this case, the robot body is stable in *rolling* direction in principle. Practically, we placed the center of mass of the robot a little bit higher than the center of the wheel arc and realized stability by control.

The other feature of the robot is that the body is separated into upper and lower parts to keep the *rolling* stability. The rotary joint between upper and lower body has an actuator to stabilize the *rolling* and to steer the body. According to the swing of the upper body, the center of mass of the robot moves. Therefore, the lower body also inclines. Finally the robot will steer itself as illustrated in Fig. 2.

Stabilization for *rolling* and *pitching* is achieved by the feedback control. Two vibration gyros which detect angular velocities around *rolling* and *pitching* axis are equipped. Measured angular velocities and pulse counts from the pulse encoders attached to axles of actuators (DC motors) are used for feedback control. We equipped another gyro to detect an angular velocity around *yawing* axis. This gyro will be used to know a "heading" direction or stabilize the body for *yawing*.

III. Experiments

A. Experimental system

The ideas described in Section II. have been realized as a robot named "Yamabico ICHIRO" (Fig. 3). It is 30 cm (D) x 30 cm (W) x 50 cm (H) in size, and weight 12 kg. This unicycle is implemented as a self-contained mobile robot which includes a controller module, internal sensors, motors and batteries on-board.

The rugby-ball-shaped wheel and the frames of the upper and lower bodies are of our own making and supported by the kind offices of Yokosuka Technical High school. Especially, the wheel was machined down by NC machining taking two days.

In a controller module, Transputer T805 is used as CPU. T805 provides us an advantage of fast floating-point calculation because it has a floating-point processor inside even though it has low power consumption characteristics. Sampling interval of control loop is 5 ms. The robot has two actuators. One DC motor (24V/20W) is for driving the wheel, and the other DC motor (24V/10W) is for *rolling* the upper side body. They are controlled by one controller module. The pulse encoders(500 pulses/revolution) are attached to the motor axles. They are used for detecting the wheel rotation angle and inclination angle between upper and lower body. One gyro to measure *pitching* angular velocity is made by Murata Co.,Ltd.,— ENC-05E, whose band-width is 50 Hz and drift is about 0.7 deg/s^2 in our experience. The other gyros to measure *rolling* and *yawing* angular velocity are Murata's,— ENV-05A, with 7 Hz band-width and with about 0.1 deg/s^2 drift. As frequency component of *pitching* is wider than that of *rolling* or *yawing*, we have to consider the trade-off between band-width and drift in

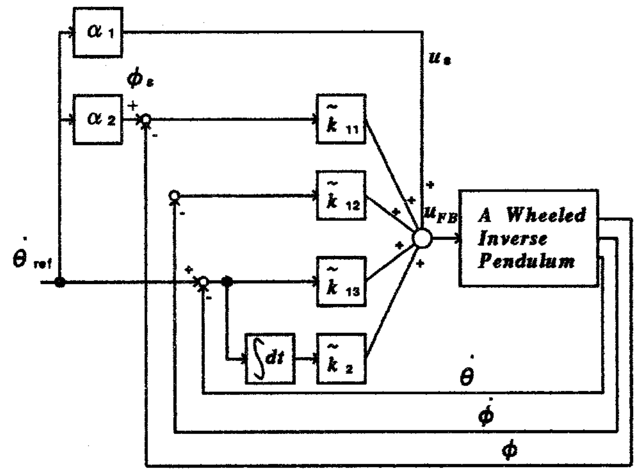

Figure 4: Block diagram of posture and locomotion velocity control for *pitching* component

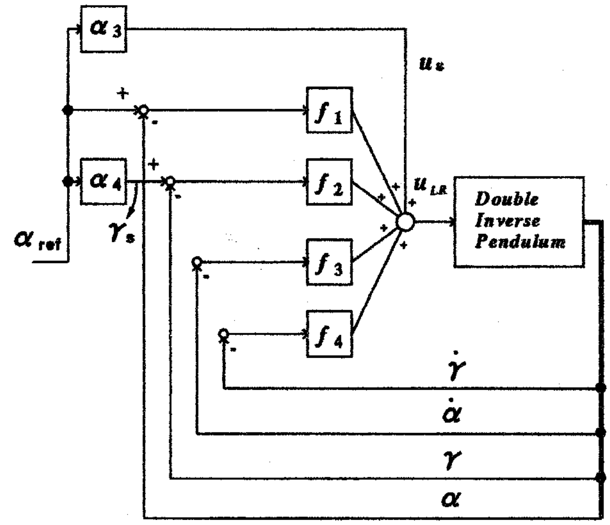

Figure 5: Block diagram of posture control system for *rolling* component

selection of the gyros.

In controller design, we have taken easier approach here, because main purpose of this paper is to present validity of proposed mechanism — to show that the mechanism has an ability to move and steer itself on the floor. We treat the dynamics around *pitching* component separately from the *rolling* component. Also, we use simple linear feedback method for stabilization in the posture and velocity control for the time being. In essence, we require rigorous and complicated analysis of dynamics, because there must be cross terms in the motion equations for proposed unicycle between the two components. However, this rigorous analysis and non-linear controller design are our next research issue in future.

Block diagram of the controller for *pitching* component is illustrated in Fig. 4 and for *rolling* component in Fig. 5. In Fig. 4, state variable ϕ and $\dot{\phi}$ are inclination angle and angular velocity of the body respectively, and $\dot{\theta}$ is a wheel rotation angular velocity (Fig. 10). This *pitching* component controller design is adopted from inverse pendulum type mobile robot [4]. As $\dot{\phi}$ measured by the gyro contains considerable drift errors, we put an observer to estimate this drift error [10], and unwanted effect caused by the drift error is avoided in stabilization of *pitching*. In Fig. 5, state variable α is an inclination angle of the lower body and γ is an angle between upper and lower bodies (Fig. 11). Feedback gains $\tilde{k}_{11}, \ldots, \tilde{k}_2$ in Fig. 4, $f_1, \ldots, f_4$ in Fig. 5, and feed-forward gains $\alpha_1, \ldots, \alpha_4$ in Fig. 4 or 5 are determined appropriately (see Appendix).

B. Experiment of the posture and velocity control in moving straight

In this section, an experimental result is presented when the unicycle moves straight. A reference velocity for a wheel is given to the controller for *pitching* component (Fig. 4), which also stabilizes the posture of the body. Simultaneously, the controller for *rolling* component regulates the angle γ and angular velocity $\dot{\gamma}$ of the joint actuator between upper and lower body into 0 *deg* and 0 *deg/s*.

A performance of this experiment is illustrated in Fig. 6 and 7. In this experiment, reference locomotion velocity is given as 0.15 m/s which competes with the wheel rotation angular velocity $\dot{\theta}_{ref}$ = 143 *deg/s*. The result represents the robot can keep its balance for both components, however a little overshoot is observed, the robot can follow the reference velocity. Convergence of the roll angles (Fig. 7) are not good for the time being. It can be improved by adjustment of feedback gain in the controller for *rolling* component.

C. Experiment of steering

The robot is expected to steer itself to follow some given trajectory on the two dimensional plane. To verify steering ability of the proposed mechanism, reference angle for the lower body (α_{ref} = 20 *deg*) is given. Then, the upper body rolls and center of the mass moves, finally contact point between the wheel and floor moves. Obviously, the robot steers itself with keeping its balance as shown in Fig. 8 and 9. In this experiment, reference locomotion velocity is also given as 0.15 m/s. Figure 9 is plotted based on the calculation by integration of *yawing* angular velocity from one gyro and by using *rolling* angle and angular velocity of the wheel.

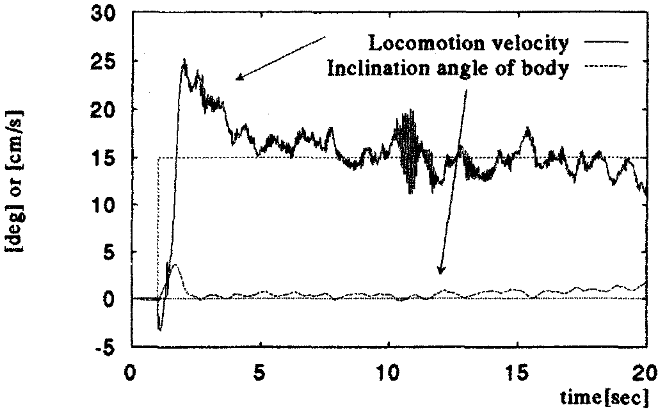

Figure 6: Experimental results of posture and velocity control — *pitching* component (Inclination angle (ϕ) and Locomotion velocity ($\dot{\theta}$))

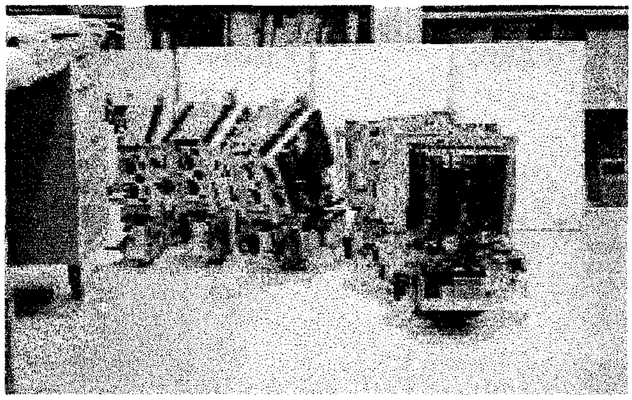

Figure 8: Synthesized snapshots picture of experiment

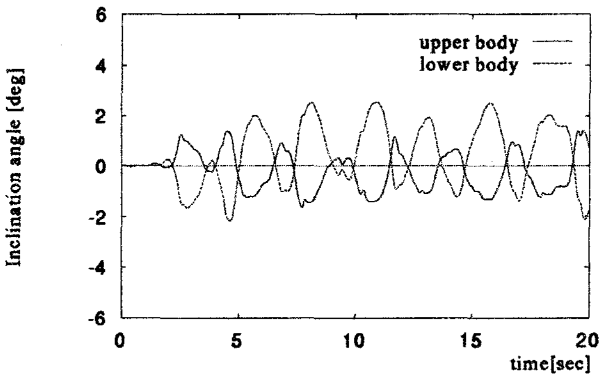

Figure 7: Experimental results of posture control — *rolling* component (Roll angle of upper body (γ) and lower body (α))

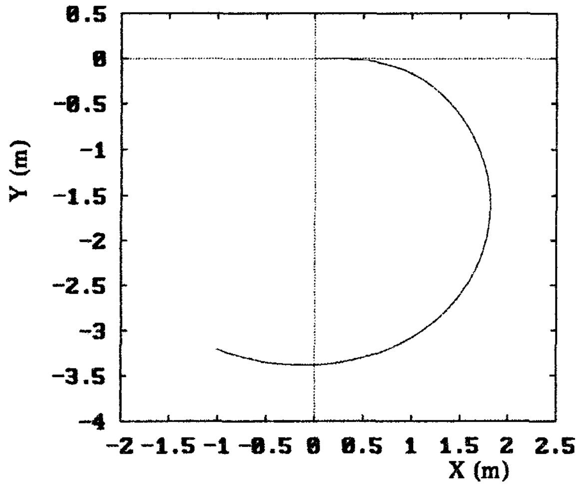

Figure 9: Experimental result of trajectory on the floor ($X - Y$) plane

IV. CONCLUSION

In this paper, we proposed a new mechanism of a unicycle robot to stabilize the posture of the robot and to steer. This robot has a large curvature wheel to help keep balance. The body of the robot is separated into the upper and lower parts, and using the roll of the upper body, the robot can stabilize its posture and steer itself. We have reported simple linear state feedback system and experimental results on the unicyle robot Yamabico ICHIRO. The robot could move on the floor at the desired velocity with keeping its balance.

Controller design based on rigorous analysis of dynamics and implementation of the trajectory controller are our future work.

Appendix

In this appendix, we present linearized equation of motions for *rolling* and *pitching* component, which are the bases for simple linear feedback controllers. As is mentioned in Section III., we took easy analysis and we have ignored cross terms among *pitching*, *rolling* and *yawing* component for the time being. Rigorous analysis for the system is a next issue of ours.

A. Controller design for pitching component

The robot can be modelled as a wheeled inverse pendulum for *pitching* component which is illustrated in Fig. 10. Parameters and variables are shown in Table 1.

We took ϕ and θ as generalized coordinates in this analysis. Equations of motion are linearized around

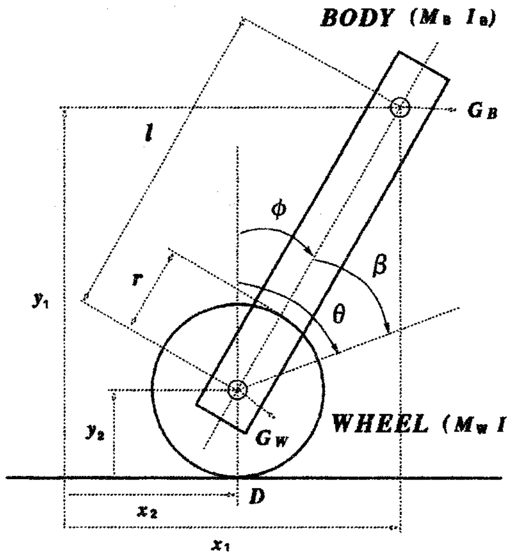

Figure 10: The model of the wheeled inverse pendulum for *pitching* component analysis

the upright posture of the robot and are obtained in the form of (1) and (2).

$$(M_Bl^2 + I_B + \eta^2 I_M)\ddot{\phi} + (M_Brl - \eta^2 I_M)\ddot{\theta} \\ +\mu_s\dot{\phi} - \mu_s\dot{\theta} - M_Bgl\phi = -\eta\tau_t u_{FB} \tag{1}$$

$$(M_Brl + M_Bl^2 + I_B)\ddot{\phi} + ((M_B + M_W)r^2 + M_Brl \\ +I_W)\ddot{\theta} + \mu_g\dot{\theta} - M_Bgl\phi = 0 \tag{2}$$

The state equation of the linearized model (3) is derived from (1) and (2).

$$\dot{\boldsymbol{X}}_{FB}(t) = \boldsymbol{A}_{FB}\boldsymbol{X}_{FB}(t) + \boldsymbol{B}_{FB}u_{FB}(t) \tag{3}$$

where,

$$\boldsymbol{X}_{FB} = \begin{pmatrix} \phi & \dot{\phi} & \dot{\theta} \end{pmatrix}^T,$$

$$\boldsymbol{A}_{FB} = \begin{pmatrix} 0 & 1 & 0 \\ a_1 & a_3 & a_5 \\ a_2 & a_4 & a_6 \end{pmatrix}, and \quad \boldsymbol{B}_{FB} = \begin{pmatrix} 0 \\ b_1 \\ b_2 \end{pmatrix}^T.$$

$a_1, \ldots, a_6, b_1$ and b_2 are coefficients which appear in (1) and (2). A linear state feedback controller for *pitching* component is designed as follows:

$$\begin{aligned} u_{FB}(t) &= u_s - \tilde{\boldsymbol{K}}\Delta\tilde{\boldsymbol{X}}_{FB}(t) \\ &= u_s - \tilde{\boldsymbol{K}}_1(\boldsymbol{X}_{FB}(t) - \boldsymbol{X}_s) - \tilde{k}_2\int_0^t(\dot{\theta}(t) - \dot{\theta}_{ref})dt \\ &= u_s - \tilde{k}_{11}(\phi(t) - \phi_s) - \tilde{k}_{12}\dot{\phi}(t) - \tilde{k}_{13}(\dot{\theta}(t) - \dot{\theta}_{ref}) \\ &\quad - \tilde{k}_2\int_0^t(\dot{\theta}(t) - \dot{\theta}_{ref})dt \end{aligned} \tag{4}$$

Table 1: Parameters and Variables for the *pitching* component

Symbol	: parameter and variable name	value[unit]
M_B	: Mass of the body	11.27[kg]
M_W	: Mass of the wheel	1.66[kg]
I_B	: Moment of inertia of the body about	0.42[kgm^2]
I_W	: Moment of inertia of the wheel about the axle	0.0029[kgm^2]
I_M	: Moment of inertia of the motor axle	1.04e-6[kgm^2]
r	: Radius of the wheel	0.06[m]
l	: Length between the wheel axle and center of mass of the robot body	0.13[m]
μ_s	: Coefficient of friction between the wheel axle including motor and gear	0.0122 [Nm/(rad/sec)]
μ_g	: Coefficient of friction between the wheel and ground	0.0458 [Nm/(rad/sec)]
η	: Reduction ratio of gear	61.54[1]
τ_t	: Torque constant of the motor	0.0235[Nm/A]
g	: Gravitational acceleration	9.8[m/s^2]
ϕ	: Inclination angle of the body	[rad]
θ	: Wheel rotation angle	[rad]
u_{FB}	: Motor input current	[A]
G_B	: The center of mass of the body	
G_W	: The center of mass of the wheel	
D	: Contact point between the wheel and the ground	

where, $\tilde{\boldsymbol{K}} = [\tilde{\boldsymbol{K}}_1, \tilde{k}_2] = [\tilde{k}_{11}, \tilde{k}_{12}, \tilde{k}_{13}, \tilde{k}_2]$ are feedback gains. u_s and ϕ_s are derived as follows:

$$u_s = \alpha_1\,\dot{\theta}_{ref} = \frac{\mu_s + \mu_g}{\eta\tau_t}\dot{\theta}_{ref},$$

and

$$\phi_s = \alpha_2\,\dot{\theta}_{ref} = \frac{\mu_g}{M_Bgl}\dot{\theta}_{ref}.$$

They are derived from (1) and (2) when $\dot{\theta}_{ref}$ is substituted for $\dot{\theta}$ and $\ddot{\phi}$, and when $\dot{\phi}$ and $\ddot{\theta}$ are assumed to be very small in the stable state. In other words, u_s is a computed (or feed-forward) torque when $\dot{\phi}$ and $\ddot{\theta}$ is expected to be zero. Actual values for α_1 and α_2 are:

$$\alpha_1 = 0.0401,\ \alpha_2 = 0.00085$$

This controller design is adopted from Ha and Yuta [4].

B. Controller design for rolling component

The robot can be modelled as one dimensional double inverse pendulum illustrated in Fig. 11 for *rolling* com-

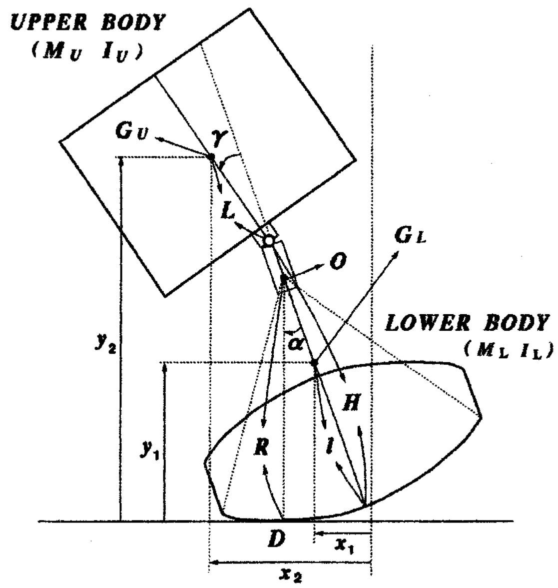

Figure 11: The model of the double inverse pendulum for *rolling* component

ponent. Let us define angles α and γ as generalized coordinates. They are illustrated in Fig. 11.

At the Joint O, there is an actuator (DC-motor) whose input current is u_{LR}. Equations of motion after linearization around the upright posture of the robot are given as follows:

$$\begin{aligned}&(M_L l^2 + M_U(H+L)^2 + I_L)\,\ddot{\alpha} + \mu_g\,\dot{\alpha}\\&+(M_L(R-l) - M_U(H-R+L))g\,\alpha\\&+M_U L(H+L)\,\ddot{\gamma} - M_U gL\,\gamma = 0,\end{aligned} \tag{5}$$

$$\begin{aligned}&M_U L(L+H)\,\ddot{\alpha} + (M_U L^2 + I_U + I_M\eta^2)\,\ddot{\gamma}\\&+\mu_s\,\dot{\gamma} - M_U gL\,\alpha - M_U gL\,\gamma = \eta\,\tau_t\,u_{LR},\end{aligned} \tag{6}$$

where all the parameters are defined in Table 2.

The state equation in the form (7) of the linearized model is derived from (5) and (6):

$$\dot{\boldsymbol{X}}_{LR}(t) = \boldsymbol{A}_{LR}\boldsymbol{X}_{LR}(t) + \boldsymbol{B}_{LR}\,u_{LR}(t), \tag{7}$$

where,

$$\boldsymbol{X}_{LR} = (\ \alpha,\ \ \gamma,\ \ \dot{\alpha},\ \ \dot{\gamma}\ )^T,$$

$$\boldsymbol{A}_{LR} = \begin{pmatrix} 0 & 0 & 1 & 0\\ 0 & 0 & 0 & 1\\ a_1 & a_3 & a_5 & a_7\\ a_2 & a_4 & a_6 & a_8 \end{pmatrix} \ \textit{and}\ \ \boldsymbol{B}_{LR} = \begin{pmatrix} 0\\ 0\\ b_1\\ b_2 \end{pmatrix}$$

$a_1, \ldots, a_8, b_1$ and b_2 are coefficients which appear in (5) and (6).

State variable $\dot{\alpha}$ is obtained by a gyro sensor which is attached on the lower body and α is derived from

Table 2: Parameters and Variables for the *rolling* component

Symbol	: parameter and variable name	value[unit]
M_U	: Mass of the upper body	4.0[kg]
M_L	: Mass of the lower body	8.4[kg]
I_U	: Moment of inertia of the upper body about the joint axle	0.115[kgm^2]
I_L	: Moment of inertia of the lower body about the joint axle	0.170[kgm^2]
I_M	: Moment of inertia of the motor axle	1.03e-6[kgm^2]
R	: Radius of the wheel(cross section)	0.20[m]
H	: Distance between the joint and the ground when the robot stands upright	0.212[m]
l	: Distance between the center of mass of the lower body and the ground when the robot stands upright	0.106[m]
L	: Distance between the joint and the center of mass of the upper body	0.128[m]
μ_s	: Coefficient of friction about motor and gear axles	0.04 [Nm/(rad/sec)]
μ_g	: Coefficient of friction between the wheel and the ground	0.02 [Nm/(rad/sec)]
η	: Reduction ratio of gear	128.0[1]
τ_t	: Torque constant of the motor	0.0438[Nm/A]
g	: Gravitational acceleration	9.8[m/s^2]
γ	: Inclination angle of the upper body	[rad]
α	: Inclination angle of the lower body	[rad]
u_{LR}	: Motor input current	[A]
G_U	: The center of mass of the upper body	
G_L	: The center of mass of the lower body	
D	:Contact point between the wheel and the ground	

integral of $\dot{\alpha}$. $\dot{\gamma}$ is measured by pulse counts of a pulse encoder of the joint motor axle during sampling time. γ is integral of $\dot{\gamma}$. A drift of gyro sensor for $\dot{\alpha}$ is ignored for the time being.

The linear state feedback controller is designed as in (8) and the block diagram is illustrated in Fig. 5.

$$\begin{aligned} u_{LR}(t) = u_s &- f_1(\alpha(t) - \alpha_{ref}) - f_2(\gamma(t) - \gamma_s) \\ &- f_3\dot{\alpha}(t) - f_4\dot{\gamma}(t) \end{aligned} \tag{8}$$

γ_s and u_s are defined as follows:

$$u_s = \alpha_3\ \alpha_{ref} = \frac{(M_L(R-l) - M_U(H-R))g}{\eta\tau_t}\alpha_{ref}$$

$$\gamma_s = \alpha_4\ \alpha_{ref} = \frac{(M_L(R-l) - M_U(H-R+L))}{M_U L}\alpha_{ref}$$

Coefficients α_3 and α_4 are derived from (5) and (6) when $\ddot{\alpha}$, $\dot{\alpha}$, $\ddot{\gamma}$ and $\dot{\gamma}$ are expected to be zero under the stable state of the robot. Where, constant value are obtained as $\alpha_3 = 0.448$, $\alpha_4 = -1.296$. $f_1, \ldots, f_4$ are feedback gains.

C. Parameter and coefficient values

Coefficient matrix $\boldsymbol{A}_{FB}$ and $\boldsymbol{B}_{FB}$ for *pitching* control are obtained by using parameters given in Table 1. as follows:

$$\boldsymbol{A}_{FB} = \begin{pmatrix} 0 & 1 & 0 \\ 29.77 & -0.244 & 0.284 \\ -46.82 & 1.242 & -1.533 \end{pmatrix}$$

$$\boldsymbol{B}_{FB} = \begin{pmatrix} 0 & -7.714 & 39.22 \end{pmatrix}^T$$

Feedback gain for $\tilde{\boldsymbol{K}}$ is given as:

$$\tilde{\boldsymbol{K}} = (-12.56, -2.46, -0.174, -0.115),$$

after optimizing calculation and *cut and try* adjustment.

On the other hand, for *rolling* control, using parameters given in Table 2, coefficient matrix $\boldsymbol{A}_{LR}$ and $\boldsymbol{B}_{LR}$ are obtained as follows:

$$\boldsymbol{A}_{LR} = \begin{pmatrix} 0 & 0 & 1 & 0 \\ 0 & 0 & 0 & 1 \\ -11.64 & 1.034 & -0.035 & 0.031 \\ 35.68 & 24.50 & 0.031 & -0.257 \end{pmatrix},$$

$$\boldsymbol{B}_{LR} = \begin{pmatrix} 0 & 0 & 8.623 & 36.00 \end{pmatrix}^T.$$

Feedback gain for (f_1, f_2, f_3, f_4) were given by pole assignment and *cut and try* adjustment as follows:

$$\boldsymbol{F} = (f_1, f_2, f_3, f_4) = (10.44,\ 15.94,\ 8.468,\ 3.047).$$

Acknowledgements

The authors thank for outstanding cooperations by educational staffs of department of the Mechanical Engineering in Yokosuka Technical High School. A part of this study in this paper is supported by Scientific Research Grant-in-aid of Japan Ministry of Education, #09750288.

References

[1] Y. Kanayama and S. Yuta : "Vehicle path specification by a sequence of straight lines," IEEE J. of Robotics and Automation, vol. 4, no. 3, pp. 265–276, 1988.

[2] S. Suzuki, J. Iijima and S. Yuta : "Design and implementation of an architecture of autonomous mobile robots for experimental researchers," 6th Int. Conf. on Advanced Robotics, pp. 423–428, 1993.

[3] S. Yuta, S. Suzuki and S. Iida, "Implementation of a small size experimental self-contained autonomous mobile robot - sensors, vehicle control, and description of sensor based behavior," R. Chatila et al. eds., Experimental Robotics II (the 2nd int. symp. on experimental robotics) pp. 344–459, Springer-Verlag, 1993.

[4] Y. Ha and S. Yuta: "Trajectory Tracking Control for Navigation of Self-Contained Mobile Inverse Pendulum," Proc. of the 1994 IEEE/RSJ int. Conf. on Intelligent Robots and Systems, pp. 1875-1882, 1994.

[5] Y. Ha and S. Yuta: "Trajectory Tracking Control for Navigation of Inverse Pendulum Type Self-Contained Mobile Robot," Journal of Robotics and Autonomous Systems, vol. 17, pp. 65–80, 1996.

[6] C. Osaka, H. Kanoh, M. Masubuchi and S. Hayashi : "Stabilization of Unicycle," System and Control, Vol.25, No.3, pp. 159-166, 1981.

[7] D. Honma, N. Iguchi, Y. Kondo, A. Michimori and H. Okubo : "One Wheel-Locomotive Robot and it's Control," Journal of the Robotics Society of Japan, Vol.2, No.4, pp. 366-371, 1984. (in Japanese)

[8] H. B. Brown, Jr and Y. Xu: "A Single Wheel, Gyroscopically Stabilized Robot," Proc. of the 1996 IEEE Int. Conf. on Robotics nad Automation, pp. 3658-3663, 1996.

[9] Z. Sheng and K. Yamafuji: "Study on the Stability and Motion Control of a Unicycle," JSME International Journal, 1994.

[10] O. Matsumoto, S. Kajita and K. Tani: "Estimation and Control of the Attitude fo a Dynamic Mobile Robot Using Internal Sensors," Journal of the Robotics Society of Japan, Vol.8, No.5, pp. 37-46, 1990. (in Japanese)